

Pulse generation of mode-locking fiber laser at 1.053 μM using graphene oxide film as saturable absorber

H. Haris^a, A. R. Muhammad^b, S. J. Tan^c, S. W. Harun^d, I. Saad^{a,*}

^a*Faculty of Engineering, Universiti Malaysia Sabah (UMS), Jalan UMS, 88400 Kota Kinabalu*

^b*Institute of Microengineering and Nanoelectronics (IMEN), Universiti Kebangsaan Malaysia (UKM), Bangi, 43600, Selangor, Malaysia*

^c*UOW Malaysia KDU University College, Utropolis Glenmarie, 40150 Shah Alam, Selangor, Malaysia*

^d*Department of Electrical Engineering, University of Malaya, 50603 Kuala Lumpur, Malaysia*

This article depicts a reliable mode-locking Ytterbium-doped fibre laser (YDFL) utilizing a saturable absorber (SA) film which was created by combining graphene oxide (GO) and polyethylene oxide (PEO) solutions. A thin film was eventually formed from the polymer composite after it was dried at room temperature. The thin film is then integrated into the YDFL cavity to initiate mode-locking process. Pulse with repetition rate of 6 MHz is observed from oscilloscope. The estimated cavity length of YDFL is calculated at approximately 25 m a total net dispersion of $-20.397 \text{ ps}^2/\text{km}$. This proves that our self-fabricated SA is successful and is proven as an effective SA.

(Received July 10, 2021; Accepted November 16, 2021)

Keywords: Saturable absorber, Ytterbium-doped fibre laser, Graphene oxide, Polyethylene oxide, Mode-locking

1. Introduction

Saturable absorber (SA) is often used to generate Q-switched and ultrashort pulsed laser in broad wavelengths. Generally, carbon-based materials such as graphene, carbon nanotube (CNT) and Silicon Germanium (SiGe) are potential candidates as SA [1] [2] [3]. Besides SA, they are widely adopted in field effect transistor (FET) for enhanced performance and reliability [4]. Graphene, a layered carbon-based material is anticipated as a replacement to silicon or at least to be integrated with silicon for silicon-based electronics devices due to its extraordinary electrical and optical properties. Contrary to carbon nanotube (CNT), the electrical properties of graphene does not depend on the chiral vector. Graphene exhibits gapless bandgap which allows absorption of light that is independent of wavelength to take place in graphene. In addition to the broad absorption of light, graphene also shows strong optical nonlinearity and sub-picosecond relaxation times which are ideal for laser mode-locking in a broad wavelengths range [5] [6]. Ultra-short pulses from fiber laser achieved using graphene SA was first demonstrated by Zhang et al., delivering pulse energy of 3nJ and pulse width of 700 fs at 1590 nm [7]. Later, graphene synthesis for mode-locked fiber laser was extensively investigated and reported using liquid-phase exfoliation (LPE), chemical vapour decomposition (CVD), carbon segregation and micro-mechanical cleavage [8] [9]. The most common and popular approach to integrate the synthesized graphene-based SA into a laser cavity is by sandwiching SA in between fiber connectors [10]. Other reported methods include free-space coupling, evanescent field interaction, and filling on the holes photonic crystal fiber (PCF) with SA solution [11] [12] [13].

Following the discovery of graphene as SA by Zhang, other derivatives of graphene such as graphene oxide (GO) had attracted the interest of researchers. Similar to graphene, GO consists of hexagonal carbon lattice structure but it also contains oxygen as functional groups. GO is adopted as SA for its strong nonlinear saturable absorption and ultra-fast relaxation [14] [15] [16].

* Corresponding author: ismail_s@ums.edu.my

One main advantage of GO is its easy handling as it has higher water dispersibility compared to graphene. [17] [18]. For the advantages mentioned above, GO is under extensive investigation in nano-electronics and photonics due to its nonlinear saturable absorption, strong electro-absorption and broadband conductance. As a result, GO is successfully proven as transparent flexible conductor, optical modulator, passive mode-locker and polarizer [19]. Other materials such as topological insulator (TI) and transition metal dichalcogenides (TMDs) are also actively investigated for pulse generation [20] [21]. In this work, soliton pulsed fiber laser was demonstrated in 1 μ m region utilizing GO as SA. The constructed soliton mode-locked pulsed fiber laser is desirable for wide range of applications, covering optical communications, biomedical imaging, and material processing [22] [23] [24].

2. Preparation and characterization of a saturable absorber based on graphene oxide

GO used in this work is synthesized from enlarged acid-washed graphite flakes using a modified Hummers technique. Below are the details of the fabrication process. Firstly, 320 mL of sulfuric acid is combined with 18g of graphite flakes (H₂SO₄), 70 mL of phosphoric acid (H₃PO₄) and 20 g of potassium permanganate (KMnO₄). After combining all the materials listed above, the mixture is then stirred using a magnetic stirrer. After all the materials are thoroughly combined through stirring process, the mixture is dried at room temperature for 3 days so that oxidation of graphite can take place. The mixture's colour slowly changes from dark purplish-green to dark brown. Later, H₂O₂ solution is added to the mixture to stop the oxidation process. The colour of the mixture is observed to change to bright yellow. This indicates that a high oxidation degree of graphite is reached. The graphite oxide is rinsed many rounds with deionized water and 1 M HCl to eliminate both chloride and sulfate ions. This process is repeated until pH of approximately 5 is achieved. The washing procedure is carried out via a simple decantation of supernatant followed by a centrifugation method with a force of 10,000 g. The GO is exfoliated during the washing process with deionized (DI) water, resulted in thickening of graphene solution and thus forming GO gel. Subsequently, the GO gel is then mixed with DI water to obtain a GO solution.

The polymer is synthesized by dissolving 2 g of PEO (average molecular weight of 1 x 10⁶ g/mol) in 200 ml of DI water using a hot plate stirrer and a magnetic stirrer. It took almost three hours to completely dissolve the PEO in DI water. The GO-PEO composite is created by dispersing a variable amount of GO-containing dispersed GO suspension into a solution of 2 g PEO in deionized water and completely mixing them using an ultra-sonification technique. To establish a stable GO-PEO composite solution, the mixer is bathed in an ultrasonic bath (a Branson 2800, 50/60 kHz) for about 2 hours. Only a small amount of the PEO solution (0.7 ml – 2.3 ml) is needed to successfully decrease GO consumption in the section. This PEO-GO combination is then allowed to cure at room temperature to produce GO-PEO film. Figure 1(a) and (b) illustrate the image of the GO-PEO film as well as the Field Emission Scanning Electron Microscope (FESEM – JSM 7600 F) image. A zoom in inspection of the GO layer created reveals neatly stratified GO, confirming the formation of GO paper [25]. EDX spectra in figure 1(c) show that the oxygen content is 44% wt and the carbon content is 56% wt.

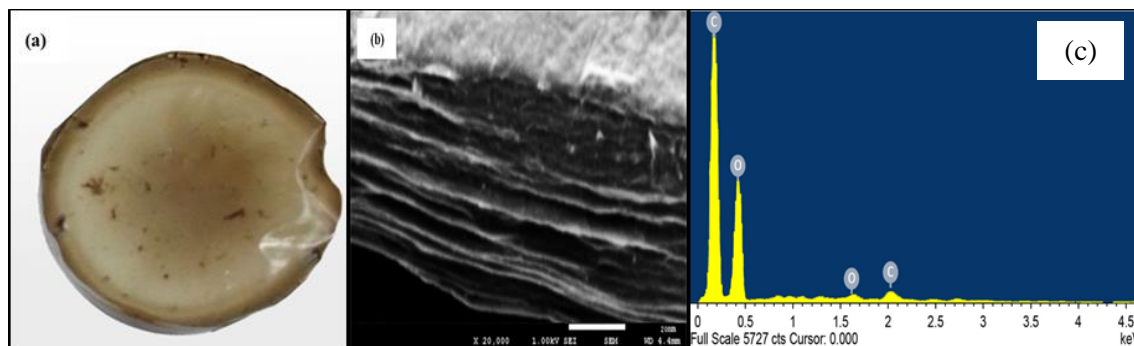


Fig. 1. Picture showing GO PEO composite film after it has dried out at room temperature. In (a), the image is real, and in (b) it is the FESEM image, and in (c) it is the EDX spectrum for the GO PEO composite film.

The Raman spectra of the manufactured GO as shown in Figure 2(a), reveals that the positions of D and G peak at 1359 cm^{-1} and 1600 cm^{-1} , respectively. The D band is caused by the defect-induced breathing mode of sp^2 rings, while the G band is caused by the first-order scattering of sp^2 carbon atoms' E_{2g} phonon. [26]. As seen in the picture, the G band of the GO has a higher frequency (of 1600 cm^{-1}) than graphite (1580 cm^{-1}) and the result tallies with the discovery given by [27]. The (ID/IG) intensity ratio for GO is calculated at 0.85. The ratio is proportional to the average size of the sp^2 clusters and relates to the measure of disorder degree [28]. Figure 2(b) shows the linear transmission spectrum for the GO film. At 1550 nm , it absorbs around 15% of the light. Figure 2(c) depicts the measured nonlinear curve of the GO-PEO film. It shows that the film exhibits 24.1 % nonlinear saturable absorption or modulation depth, 72 MW/cm^2 saturable intensity, and 35.1 % non-saturable absorption.

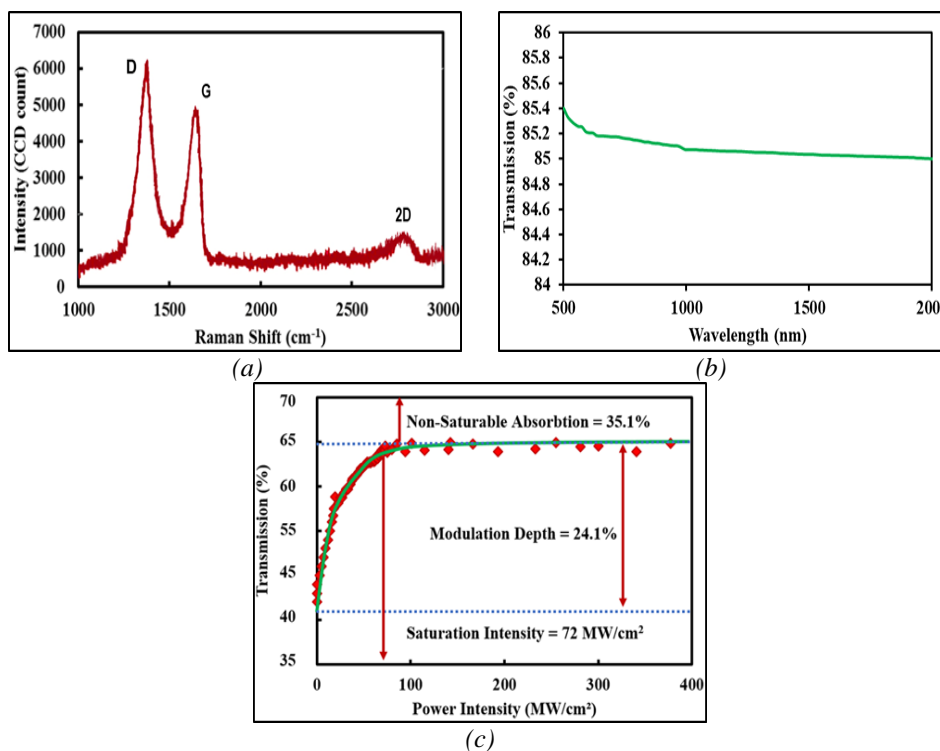


Fig. 2. Characterization of GO film; (a) Raman spectrum, (b) Linear transmission spectrum, and (c) Nonlinear transmission characteristic.

3. GO PEO film as SA is used as the configuration of the mode-locked Ytterbium-doped fibre laser

Figure 3(a) depicts the laser cavity in a ring configuration. The gain medium used 1m long Ytterbium-doped fiber (YDF). The characteristics of The YDF (Yb1200-4/125) is as follows: core diameter: 4 μ m, cladding diameter: 125 μ m, numerical aperture (NA): 0.20, cut-off wavelength: 1010 nm, Ytterbium ion absorption: 280 dB/m at 920 nm and group velocity dispersion (GVD): 24.22 ps²/km. The remaining of the cavity consists of single-mode fiber (HI 1060) with a GVD of -21.9 ps²/km. YDF is pumped by a 980 nm laser diode (LD) via a 980/1064 nm wavelength division multiplexer (WDM). The SA is assembled by careful placement of graphene PEO in between two fiber ferrule. Index matching gel is applied to the ferrule to ensure that the SA film sits firmly at the middle of core region at the fiber end. Another purpose of employing index matching gel is to minimize the insertion loss. The insertion loss of the SA device is measured to be around 4 dB at 1050 nm region. The total net dispersion and length of the laser cavity is estimated at 35.025 ps/km.nm and 25 m, respectively.

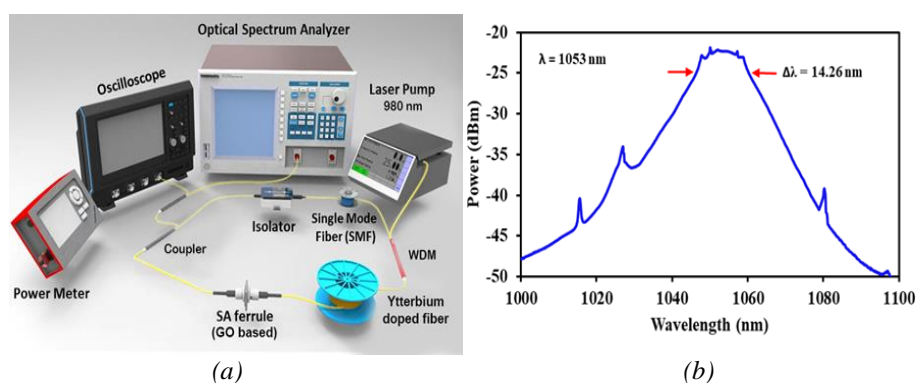


Fig. 3. (a) Experimental set-up using GO PEO film as SA in mode-locked YDFL (b) Output spectrum of the mode-locked YDFL

An isolator is positioned within the laser cavity so that light in the cavity propagates only in one direction, while the function of polarization controller (PC) is to adjust the polarization state of light for optimized mode-locking operation. A portion of the light from the constructed laser cavity is coupled out via a 90/10 coupler for monitoring purpose. A 3dB coupler which is placed at the 10% port of 90/10 coupler further splits the output light into two. One port of the 3dB coupler is linked to optical spectrum analyzer (OSA, Yokogawa AQ6370B), with resolution of 0.02 nm and the other port is connected to Oscilloscope (LeCroy,352A) and 7.8 GHz radio frequency spectrum analyzer (RFSA, Anritsu MS2683A). The characteristics of pulse in the time domain is analyzed using oscilloscope via a 1.2 GHz InGaAs photodetector.

It is observed that mode-locking is initiated when the pump power is gradually increased to 81.5 mW. Figure 3(b) shows the obtained typical mode-locked soliton spectrum with distinctive Kelly side-bands obtained from OSA when the 980 nm pump power is further increased to 204.5 mW. The center operating wavelength of the soliton is ascertained at 1054 nm with full width half maximum (FWHM) of 14.26 nm. It is noted that the spectrum broadens with the increment of pump power due to self-phase modulation (SPM) effect. The pulse width is determined using the time-bandwidth product (TBP) equation by fitting the calculated pulse to sech² pulse profile of 0.315 based on the characteristics of the laser cavity and measured FWHM value of 14.26 nm [29]. The calculation reveals that a minimum possible pulse width is of 0.08 ps.

4. GO-PEO SA mode-locking pulse generating

Figure 4(a) and (b) show the characteristics of pulse train recorded from oscilloscope under the pump power of 214.5 mW. As can be seen from Figure 4(a), the mode-locking operation

is stable under laboratory condition, with small amplitude variation at the pulse train. A zoom in view with time span of 1500 ns on the pulse train is as illustrated in Figure 4(b). The period of pulse train was measured to be around 165 and this translated to a repetition rate of 6 MHz. The obtained fundamental repetition rate tallies with the total cavity length of 25 m. The RF spectrum of the mode-locking pulse is described in Figure 4(c). The output observed at RF spectrum analyzer revealed a prominent peak at 6 MHz with signal to noise ratio (SNR) of 66 dB. As can be seen in Figure 4(b), the relationship between output power and pulse energy are found to be increasing with pump power. Pulse output power is measured with power meter and it is found to be increasing with pump power. At 214.5 mW pump power, the maximum output power is measured around 12.1 mW. On the other hand, the same increasing trend is also observed for pulse energy. The calculated pulse energy increased from 6.2 nJ (110.5 mW) to 1.5 nJ (214.5 mW). It is noted that beyond the pump power 214.5 mW, no pulse is detected.

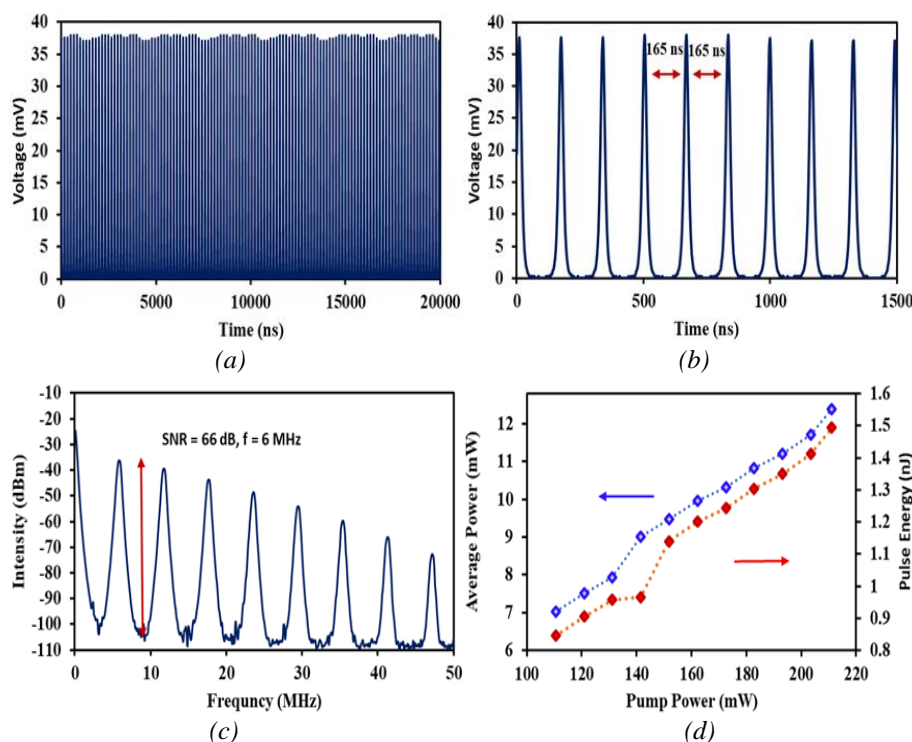


Fig. 4. Pulse train of the mode-locked YDFL at the pump power of 214.5 mW at time spans of (a) 20 000 ns (b) 15000 ns. (c) RF spectrum of the mode-locked YDFL and (d) Average output power and pulse energy with respect to 980 nm pump power for the mode-locked YDFL.

5. Conclusion

A low cost soliton mode-locked YDFL was successfully constructed and demonstrated using self-prepared GO SA. It operates at 1053 nm region with repetition rate of 6.0 MHz and stable at SNR of 66 dB. The calculated pulse width and pulse energy are 0.08 ps and 1.5 nJ, respectively. This work proves that the self-fabricated GO SA is successful to be used as a SA in the 1- μ m region to generate stable ultrashort pulse.

Acknowledgements

The authors would also like to thank the research facility from Universiti Malaysia Sabah (UMS) for supporting this research under Niche Research Fund Scheme (SDN), grant no. SDN00286, Postgraduate Research Grant Scheme (UMSGreat), grant no. GUG0444-1/2020, and

Postgraduate Assistance Scheme (SBP) and Photonics Engineering Laboratory, University of Malaya, for the research facility provided throughout this work.

References

- [1] A. K. J. s. Geim, "Graphene: status and prospects," vol. 324, no. 5934, pp. 1530-1534, 2009.
- [2] E. Singh, R. Srivastava, U. Kumar and A. D. J. N. N. R. Katheria, "Carbon nanotube: A review on introduction, fabrication techniques and optical applications," vol. 4, pp. 120-126, 2017.
- [3] D. Pogaku and I. Saad, "Effects of S/D doping concentrations on strained SiGe vertical I-MOS characteristics," in *2011 3rd International Conference on Electronics Computer Technology*, 2011, vol. 2, pp. 294-297: IEEE.
- [4] M. T. Ahmadi, Y. W. Heong, I. Saad and R. Ismail, "MOSFET-Like carbon nanotube field effect transistor model," in *Nanotech Conference &*, 2009.
- [5] Z. Sun, T. Hasan, A. J. P. E. L.-d. S. Ferrari and Nanostructures, "Ultrafast lasers mode-locked by nanotubes and graphene," vol. 44, no. 6, pp. 1082-1091, 2012.
- [6] Z. Sun, T. Hasan, F. Torrisi, D. Popa, G. Privitera, F. Wang, F. Bonaccorso, D. M. Basko and A. C. J. A. n. Ferrari, "Graphene mode-locked ultrafast laser," vol. 4, no. 2, pp. 803-810, 2010.
- [7] H. Zhang, Q. Bao, D. Tang, L. Zhao and K. J. A. P. L. Loh, "Large energy soliton erbium-doped fiber laser with a graphene-polymer composite mode locker," vol. 95, no. 14, p. 141103, 2009.
- [8] F. Bonaccorso, Z. Sun, T. Hasan and A. J. N. p. Ferrari, "Graphene photonics and optoelectronics," vol. 4, no. 9, pp. 611-622, 2010.
- [9] R. Ganatra and Q. J. A. n. Zhang, "Few-layer MoS₂: a promising layered semiconductor," vol. 8, no. 5, pp. 4074-4099, 2014.
- [10] H. Haris, S. Harun, C. Anyi, A. Muhammad, F. Ahmad, S. Tan, R. Nor, N. Zulkepely, N. Ali and H. J. J. o. M. O. Arof, "Generation of soliton and bound soliton pulses in mode-locked erbium-doped fiber laser using graphene film as saturable absorber," vol. 63, no. 8, pp. 777-782, 2016.
- [11] D. Sun, G. Aivazian, A. M. Jones, J. S. Ross, W. Yao, D. Cobden and X. J. N. n. Xu, "Ultrafast hot-carrier-dominated photocurrent in graphene," vol. 7, no. 2, pp. 114-118, 2012.
- [12] S. Tan, H. Haris, X. Cheng and S. Harun, "Mode-locked Pulsed Fiber Laser with Graphene Solution as Saturable Absorber Deposited in Photonic Crystal Fiber," in *2019 18th International Conference on Optical Communications and Networks (ICOON)*, 2019, pp. 1-3: IEEE.
- [13] Y.-H. Lin, C.-Y. Yang, J.-H. Liou, C.-P. Yu and G.-R. J. O. e. Lin, "Using graphene nanoparticle embedded in photonic crystal fiber for evanescent wave mode-locking of fiber laser," vol. 21, no. 14, pp. 16763-16776, 2013.
- [14] Q. Bao, H. Hoh and Y. Zhang, *Graphene Photonics, Optoelectronics, and Plasmonics*. CRC Press, 2017.
- [15] M. Gu, Q. Zhang and S. J. N. R. M. Lamon, "Nanomaterials for optical data storage," vol. 1, no. 12, pp. 1-14, 2016.
- [16] G. Sobon and J. J. C. N. Sotor, "Recent Advances in Ultrafast Fiber Lasers Mode-locked with Graphenebased Saturable Absorbers," vol. 12, no. 3, pp. 291-298, 2016.
- [17] P. Matyba, H. Yamaguchi, G. Eda, M. Chhowalla, L. Edman and N. D. J. A. N. Robinson, "Graphene and mobile ions: the key to all-plastic, solution-processed light-emitting devices," vol. 4, no. 2, pp. 637-642, 2010.
- [18] S. Yin, Y. Zhang, J. Kong, C. Zou, C. M. Li, X. Lu, J. Ma, F. Y. C. Boey and X. J. A. N. Chen, "Assembly of graphene sheets into hierarchical structures for high-performance energy storage," vol. 5, no. 5, pp. 3831-3838, 2011.

- [19] J. Lee, J. Koo, P. Debnath, Y. Song and J. J. L. P. L. Lee, "A Q-switched, mode-locked fiber laser using a graphene oxide-based polarization sensitive saturable absorber," vol. 10, no. 3, p. 035103, 2013.
- [20] H. Haris, H. Arof, A. R. Muhammad, C. L. Anyi, S. J. Tan, N. Kasim and S. W. Harun, "Passively Q-switched and mode-locked Erbium-doped fiber laser with topological insulator Bismuth Selenide (Bi₂Se₃) as saturable absorber at C-band region," *Optical Fiber Technology*, vol. 48, pp. 117-122, 2019.
- [21] N. Kadir, E. I. Ismail, A. A. Latiff, H. Ahmad, H. Arof and S. W. Harun, "Transition metal dichalcogenides (WS₂ and MoS₂) saturable absorbers for mode-locked erbium-doped fiber lasers," *Chinese Physics Letters*, vol. 34, no. 1, p. 014202, 2017.
- [22] J. Bliedtner, C. Schindler, M. Seiler, S. Wächter, M. Friedrich and J. J. L. T. J. Giesecke, "Ultrashort Pulse Laser Material Processing: An extension of application variety for ultrashort pulse laser processing of different materials," vol. 13, no. 5, pp. 46-50, 2016.
- [23] Y. Zhao, P. Guo, X. Li and Z. J. C. Jin, "Ultrafast photonics application of graphdiyne in the optical communication region," vol. 149, pp. 336-341, 2019.
- [24] T. Wang, P. D. Kumavor and Q. J. J. o. b. o. Zhu, "Application of laser pulse stretching scheme for efficiently delivering laser energy in photoacoustic imaging," vol. 17, no. 6, p. 061218, 2012.
- [25] D. A. Dikin, S. Stankovich, E. J. Zimney, R. D. Piner, G. H. Dommett, G. Evmenenko, S. T. Nguyen and R. S. J. N. Ruoff, "Preparation and characterization of graphene oxide paper," vol. 448, no. 7152, pp. 457-460, 2007.
- [26] A. C. Ferrari and D. M. J. N. n. Basko, "Raman spectroscopy as a versatile tool for studying the properties of graphene," vol. 8, no. 4, pp. 235-246, 2013.
- [27] K. N. Kudin, B. Ozbas, H. C. Schniepp, R. K. Prud'Homme, I. A. Aksay and R. J. N. I. Car, "Raman spectra of graphite oxide and functionalized graphene sheets," vol. 8, no. 1, pp. 36-41, 2008.
- [28] G. Sobon, J. Sotor, J. Jagiello, R. Kozinski, M. Zdrojek, M. Holdynski, P. Paletko, J. Boguslawski, L. Lipinska and K. M. J. O. e. Abramski, "Graphene oxide vs. reduced graphene oxide as saturable absorbers for Er-doped passively mode-locked fiber laser," vol. 20, no. 17, pp. 19463-19473, 2012.
- [29] C. J. D. o. P. U. o. R. Antoncini, "Ultrashort laser pulses," pp. 1-35, 2014.